Journal of Basic & Clinical Medicine

http://www.sspublications.org/index.php/JBCM/index

Ratiometric Anion Sensing Based on Inhibition of Excited-state Intramolecular Proton Transfer: the Role of Additional -NH Binding Site

Yunkou Wu[1,2], Jiangli Fan[1] and Xiaojun Peng[1]*

[1]State Key Laboratory of Fine Chemicals, Dalian University of Technology, Dalian, China; [2]Russell H. Morgan Department of Radiology and Radiological Science, Johns Hopkins University School of Medicine, Baltimore, Maryland

Journal of Basic & Clinical Medicine 2017; 6(2):12-20

Abstract

Two new fluorescent sensors, PUTO and PUIO, were designed for recognition of anions based on the mechanism of inhibiting the Excited-State Intramolecular Proton Transfer (ESIPT). New sensors were synthesized by condensing phenyl isocyanate with 2-(2'-aminophenyl)benzothiazole and 2-(2'-aminophenyl)benzimidazole, respectively. Superior anion sensitivity was observed in PUIO, which might be owing to the additional -NH binding site of the imidazole ring in its structure to enhance the ESIPT efficiency. Among the anions with similar basicity and surface charge density (F^-, $CH_3CO_2^-$ and $H_2PO_4^-$), F^- forms the strongest hydrogen bond with PUIO. PUIO-F^- hydrogen bonding interactions could efficiently inhibit the ESIPT process, which might give a sensitive ratiometric response in fluorescence.

Key Words: Florescence, anion sensing, excited-state intramolecular proton transfer, hydrogen bonding

Introduction

For the hydrogen bond donor groups (-OH, -NH2, etc.) and the hydrogen bond acceptor groups (=N-, >C=O, etc.), if these groups conjugate with the aromatic rings, their hydrogen bond donor or acceptor abilities increase significantly in excited-state. As a consequence, molecules with the intramolecular hydrogen bonds (IHB) between pairs of these groups often experience excited-state intramolecular proton transfer (ESIPT) process from hydrogen bond donors to acceptors (1, 2). Normally, the formed phototautomers can emit fluorescence with a large Stokes shift of more than 10000 cm^{-1}, so molecules with ESIPT capacity often possess dual fluorescence bands: the small Stokes shift of normal bands and the large Stokes shift of tautomer bands (1). Due to the interesting nature of the ESIPT process and the desirable spectral properties of ESIPT molecules, significant efforts have been made to develop the cation sensors based on inhibition of ESIPT process (3-7), however, there has been a paucity of reports of anion sensors based on inhibition of ESIPT mechanism (8, 9).

Received: November 6, 2017; Accepted: November 20, 2017
*Correspondence author: Dr. Xiaojun Peng, State Key Laboratory of Fine Chemicals, Dalian University of Technology
2 Linggong Road, Dalian 116024, PR China.
Tel: +86-411-84986306; E-mail: pengxj@dlut.edu.cn

In view of the importance of detection and quantification of anions in disciplines such as biology and environmental science (10, 11), considerable efforts have been made to design fluorescent sensors for anions by utilizing various mechanisms such as internal charge transfer (ICT) (12), photo-induced electron transfer (PET) (13, 14), metal-to-ligand charge transfer (MLCT) (15), excimer/exciplex formation (16), and tuning proton transfer (17). We had systemically studied the anion sensing based on inhibition of ESIPT mechanism a few years ago (18). Interestingly, for the urea-receptor contained sensor PUBO in Scheme 1, it exhibits different spectral outputs in the presence of basic anions such as F^-, $CH_3CO_2^-$ and $H_2PO_4^-$ because of the different mechanisms and degrees for ESIPT inhibition. However, the sensitivity of PUBO for anion sensing is low because it needs a relative large amount of anions to efficiently inhibit the ESIPT process in PUBO. In addition, the low ESIPT efficiency of PUBO also leads to the low detection sensitivity (18). Therefore, further improvements should be made to increase the detection sensitivity for the urea-receptor contained ESIPT sensors.

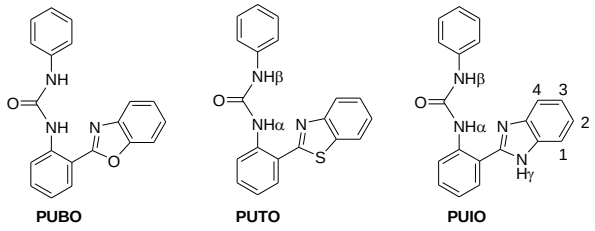

Scheme 1. Structures of sensors PUBO, PUTO and PUIO.

In the present study, in order to increase the detection sensitivity of sensor for anions, new structures were developed by replacing the benzoxazole moiety in PUBO with the benzothiazole and benzimidazole to give PUTO and PUIO, respectively (Scheme 1). In particular, the differences in π-donor and σ-acceptor properties between sulfur and oxygen atom resulted in a more acid receptor in PUTO than that of PUBO, so it is expected that PUTO will have a stronger affinity to anions than PUBO (19). For PUIO, the additional -NH binding site of the imidazole ring possibly plays a role in hydrogen bonding with anions, so it is expected that PUIO possibly forms a stronger hydrogen bond interactions with anions, and indeed, interesting results were obtained after a detail investigation about PUIO-anion interactions in this work.

Table 1. UV/Vis spectral data (absorption maxima and extinction coefficients) and fluorescence spectral data (λ_{ex} = 340 nm) for PUTO and (λ_{ex} = 325 nm) for PUIO in various solvents

sensor	solvent	λ_{max} (nm)	ε_{max} ($M^{-1}cm^{-1}$)	λ_{max} (nm)	ε_{max} ($M^{-1}cm^{-1}$)	λ_{max}^{fl} (N) [a]	Φ_{fl} (N) [a]	λ_{max}^{fl} (T) [b]	Φ_{fl} (T)
PUTO	toluene	296	14627	352	12651	405	0.005	586	0.009
	DCM	296	13570	345	12312	382	0.018	571	0.010
	acetonitrile	293	15001	343	13463	402	0.015	571	0.004
	DMSO	296	15541	348	12337	415	0.015	582	0.004
	ethanol	293	14387	343	12428	403	0.006	574	0.007
	methanoll	293	15730	341	13829	410	0.013	576	0.005
PUIO	toluene	303	17500	330	16400	-	-	519	0.23
	DCM	303	16300	328	15500	-	-	515	0.21
	acetonitrile	301	17200	322	16200	-	-	513	0.26
	DMSO	303	18100	326	17100	-	-	516	0.28
	ethanol	302	17900	324	16900	-	-	507	0.32
	methanoll	301	17400	322	16000	-	-	506	0.29

[a]N = normal band, which cannot be accurately detected for PUIO; [b]T = tautomer band.

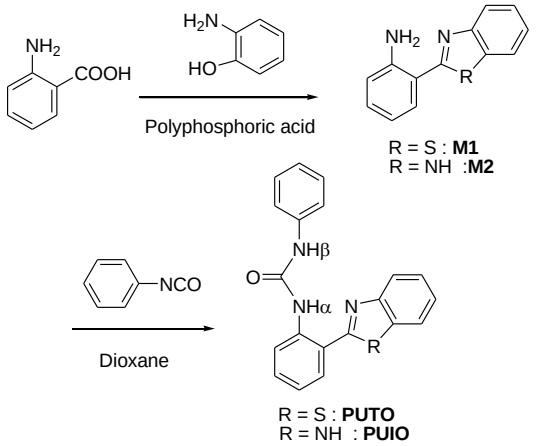

Scheme 2. Procedures for synthesizing new sensors PUTO and PUIO.

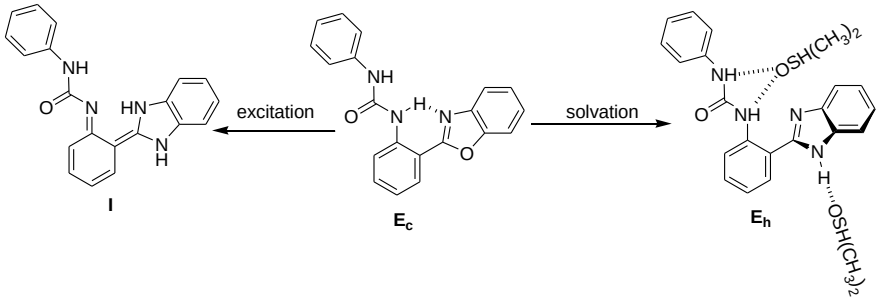

Scheme 3. Possible forms of PUIO in the ground state and the excited state.

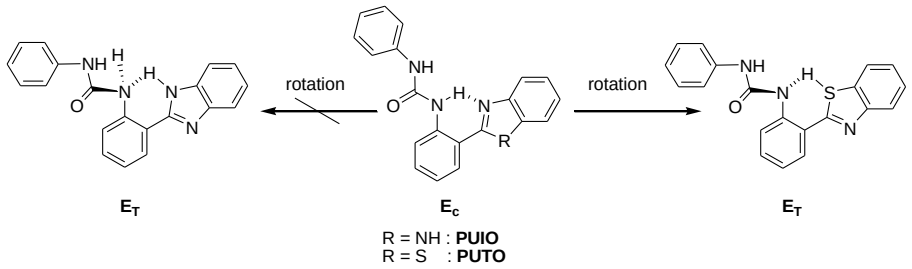

Scheme 4. The rotamers of PUBO and PUIO in solutions.

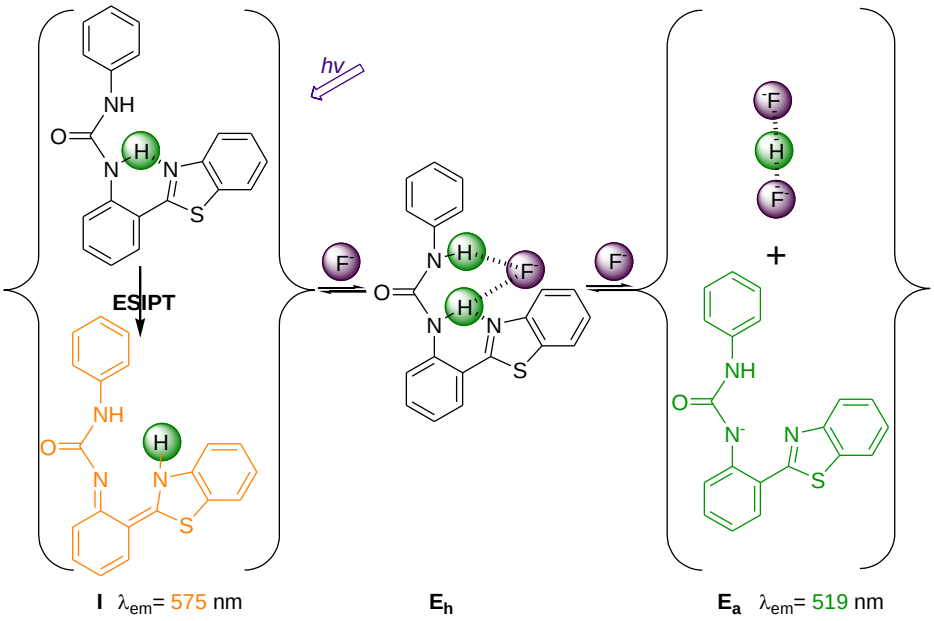

Scheme 5. Inhibition of ESIPT in PUTO by F^-.

Results and Discussion

Synthesis

The syntheses of PUTO and PUIO are shown in Scheme 2. First, the 2-(2'-aminophenyl)benzothiazole **M1** and 2-(2'-aminophenyl)benzimidazole **M2** were prepared in 95 % and 60 % yields, respectively, according to literature method (20), then condensation of them with phenyl isocyanate in dry dioxane gave PUTO and PUIO, respectively, in ~80% yield.

Photophysics of sensors

The photophysical properties of PUTO and PUIO were investigated in various solvents. The absorption spectra of them were structured in different solvents, indicating the rigidity of their molecular frameworks. Their absorption band maxima underwent slight blue shifts with the increase of the polarity and hydrogen bond capacity of the solvents (Table 1), which may be due to the results of the partial broken of the IHB with the formation of the NHα-solvent hydrogen-bond complex E_h (Scheme 3) (21).

The fluorescence spectral data of PUTO and PUIO were also measured in different solvents (Table 1). Interestingly, there are big differences for the emission pattern between PUTO and PUIO when the excitation wavelengths are chosen in their absorbance maxima. For example, PUTO possessed dual emission bands when the excitation was chosen at 345 nm in DMSO (Figure 1): the small Stokes shifted band of normal emission at 409 nm and the large Stokes shifted band of tautomer emission at 575 nm. The intensity of the tautomer band was small when compared with that of the normal band. On the other hand, PUIO only gave a single emission band at 516 nm (Figure 1), when the excitation was chosen at 326 nm. The large Stokes shift of more than 11100 cm^{-1} and the independence of the excitation wavelengths for this single emission band in PUIO indicate that it belongs to the tautomer emission and derives from the tautomer species I (Scheme 3). A very weak normal emission band of PUIO could be detected only when the excitation was chosen at a short wavelength (300 nm) and the normal band of PUIO was very small when compared with that of PUTO.

A simple rotation of the carbon bond that links the phenyl and thiazole ring will change the cis-rotamer $\mathbf{E_C}$ of PUTO to the trans-rotamer $\mathbf{E_T}$ (Scheme 4). Similar to PUBO, the normal emission band of PUTO derives from the excitation of the trans-rotamer $\mathbf{E_T}$

and the solvated species Eh, while the tautomer emission band of PUTO derives from the excitation of the cis-rotamer $\mathbf{E_C}$ (18). However, for PUIO, the trans- and cis-rotamer are expected to be very different in energy (Scheme 4). The analogous $\mathbf{E_C}$ structure for PUIO requires the rehybridization of the urea nitrogen, which accompanies with the loss of resonance stabilization energy between the urea nitrogen lone pair and the phenyl moiety. As a result, the $\mathbf{E_C}$ is thermodynamically and substantially favored over the $\mathbf{E_T}$ in PUIO, therefore, the ground-state equilibrium for PUIO is expected to be dominated by a single rotamer $\mathbf{E_C}$ and the solvated species $\mathbf{E_h}$ (Scheme 3). This is the reason why there exists a very small normal band in PUIO, while more $\mathbf{E_C}$ is available to give the tautomer band. The quantum yield of the tautomer emission in PUIO (0.28 in DMSO, Table 1) is quite high when compared with that of the PUTO (0.004 in DMSO, Table 1). In addition, as only rotamer $\mathbf{E_C}$ dominates in the ground-state equilibrium in PUIO, there is a less chance of the occurrence of nonradiative decay because of the rotation in the excited state (22), which also contributes to the increase of the quantum yield in PUIO. On the basis of the above discussions, it is found that it is the additional -NH binding site of the imidazole ring in PUIO that results in the increasing of the ESIPT efficiency and quantum yields, which can also play an important role in enhancing the anion detection sensitivity.

Anion inhibition of ESIPT in PUTO and PUIO

Sensor-anion interactions were investigated through spectrophotometric titrations by adding a standard solution of the tetrabutylammonium salt of anions to a dry DMSO solution of sensors. Figure 2 shows the UV/Vis spectral changes of PUTO during the titration with F^-. Addition of F^- induces the stepwise changes in absorbance: the first step is the slight increase in charge transfer band at 425 nm with the addition of F^- up to 60 molar equivalents, and the maximum absorbance band at 347 nm does not change; the second step is the decrease of the maximum absorbance band at 347 nm accompanying the increase of the charge transfer band at 425 nm and there appears well-defined isosbestic points at 332 nm and 374 nm, respectively. Similar to its UV/Vis spectral changes, the fluorescence titration spectra of PUTO also exhibit stepwise changes: first, the normal emission band increases slightly with the addition of F^-, then there appears a large charge transfer emission band, which lies between the normal and tautomer emission band and buries them quickly with the addition of F^-. The above spectral changes during F^- titration are consistent with those of PUBO (18). Considering the similar structure between PUTO and PUBO, it is deduced that PUTO interaction pattern with F^- is similar to that of PUBO, and the process for F^- inhibition of ESIPT in PUTO is illustrated in the Scheme 5: the first step is the PUTO-F^- hydrogen-bond complex formation process. This step produces minimal disturbance on the dipole associated with the charge-transfer transition in PUTO. Therefore, only a small change is observed in the spectra (Figure 2a). The second step is the F^--induced deprotonation of Hα to form the $\mathbf{E_C}$. With the charge redistribution taking place within the deprotonated species in this step, the UV/Vis and fluorescence spectra exhibit a red shifted CT band. The fluorescent titration experiment (Figure 3) indicates that it is the deprotonation that efficiently inhibits the ESIPT process in PUTO, which gives a proton-dissociation constant (log K_d) of 2.51 ± 0.10 for the deprotonation, a value larger than that of PUBO (log K_d = 2.09 ± 0.08), indicating the difference in π-donor and σ-acceptor properties between sulfur and oxygen atom indeed results in a more acidic receptor in PUTO, and makes PUTO more sensitive to F^-. In fact, sulfur's role in enhancing the acidity of sensors has been reported in many studies (19, 23, 24). Replacing the oxygen in PUBO with the sulfur atom in PUTO can significantly increase in the anion detection sensitivity in PUTO. While it should be noted that the low ESIPT efficiency in PUTO will limit its utilization as a sensitive ESIPT sensor.

The spectral changes for PUIO-F^- interactions are different from those of the PUTO. Addition of F^- induces the decrease of the maximum absorbance band at 326 nm and the appearance of two well-defined isosbestic points at 306 nm and 288 nm, respectively (Figure 4a). From the above discuss, it is known that F^- is a strong base that has a strong ability to deprotonate the anion sensors (17, 25). However, the absence of red-shift charge-transfer band that results from deprotonation even in the presence of excess of F^- indicates F^- can only form hydrogen bonding interaction with PUIO during the entire titration.

^{1}H NMR titration experiments in DMSO-d_6 were conducted to disclose the complexation pattern for PUIO-F^- interactions. It should be noted that two effects are responsible for the ^{1}H signal changes upon NH-anion hydrogen-bond formation: 1) The bond effects increase the electron density of the phenyl ring and therefore promote an upfield shift; and 2) the space effects can polarize C-H bond in proximity to hydrogen bonding, and in turn create partial positive charge on the proton, and eventually cause a downfield shift (25). Upon addition of 0.5 molar equivalents of F^-, the complete disappearance of the signals of the urea proton Hα (12.0 ppm) and imidazole proton Hγ (13.1 ppm) was observed, indicating these protons form strong hydrogen bond with F^- (Figure 5). On the basis of the pattern of the spectral changes with the further addition of F^- from 1 to 4 molar equivalents, the protons can be classified as two categories (Figure 5): the first category is the protons that shift to downfield with the addition of F^-, while the second is those shifting to upfield. For the protons that are in close proximity to site of hydrogen bonding (such as proton 1), the through-space effects dominate, so the downfield shifting of the first group of protons is observed. However, for the protons that are far away from the site of hydrogen bonding (such as proton Hβ, 2, 3 and 4), the through-bond effects take action and the protons shift upfield. On the basis of the above analysis, the hydrogen bonding pattern for PUIO-F^- interaction is illustrated in Scheme 6. With the addition of F^-, urea proton Hα and imidazole proton Hγ form strong hydrogen bonding with F^-. This intermolecular hydrogen bonding is strong enough to break the IHB that is critical to the occurrence of ESIPT. With the destroying of the rigidity of the cis-rotamer $\mathbf{E_C}$, the blue shift and decrease in the maximum absorption band at 326 nm are observed during the titration (Figure 4a).

From the above absorbance and ^{1}H NMR titration results, it is found that PUIO-F^- interaction in the ground state is a hydrogen bonding process, which disturbs the IHB and induces the conformation change in PUIO, so it is expected that ESIPT process will be affected by F^- binding. Indeed, the ESIPT in PUIO can be efficiently inhibited by F^-. With the addition of F^-, the tautomer band at 516 nm decreases gradually accompanying the increase of a new band at 450 nm (Figure 4 and Figure 6), and this new band is ascribed to the PUIO-F^- hydrogen-bond complex according to the above discussions. It has been known that the anion sensitivities of PUBO and PUTO are relative low (log K_d of 2.09 ± 0.08 for PUBO and 2.51 ± 0.10 for PUTO) because efficient inhibition of ESIPT in them by F^- can only occur in the deprotonation process. However, in the case of PUIO, the ESIPT can be efficiently inhibited during the hydrogen bonding process. Therefore, a relative large log K_a value of 3.10 ± 0.02 was observed from the fluorescent titration spectra, indicating PUIO has a better detection sensitivity for F^-. Besides the large log K_a

value, two other factors may also contribute to enhancing the sensitive detection of F^- with PUIO. The first factor is the ratiometric change of the fluorescence in response to the F^-. The ratiometric response nature can increase the detection sensitivity because ratiometric response is independent on the concentration of the sensor, the fluctuation of source-light intensity, and the sensitivity of instrument (26). The second factor is the high ESIPT efficiency and high quantum yield in PUIO. So the additional hydrogen bond donor from the imidazole ring in PUIO plays a critical role in controlling the F^- sensing process, in enhancing the ESIPT efficiency and therefore in increasing the F^- detection sensitivity.

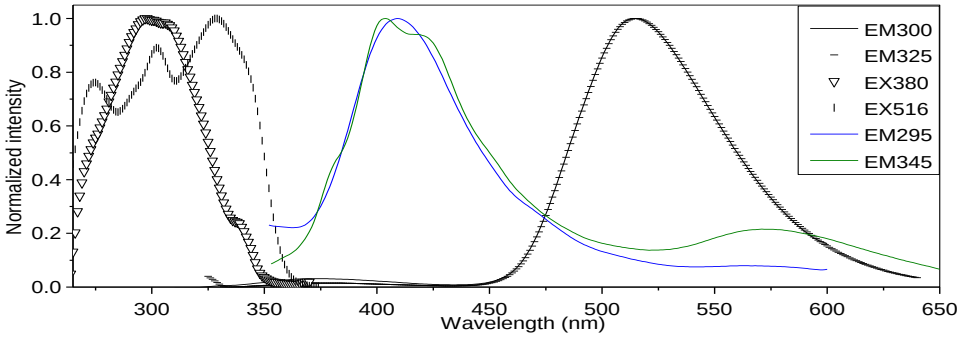

Fig. 1. The normalized fluorescent excitation (Ex) and emission (Em) spectra for PUIO (black) and PUTO (color line) in DMSO, and the indicated wavelengths (nm) refer to the wavelengths at which the spectra are recorded.

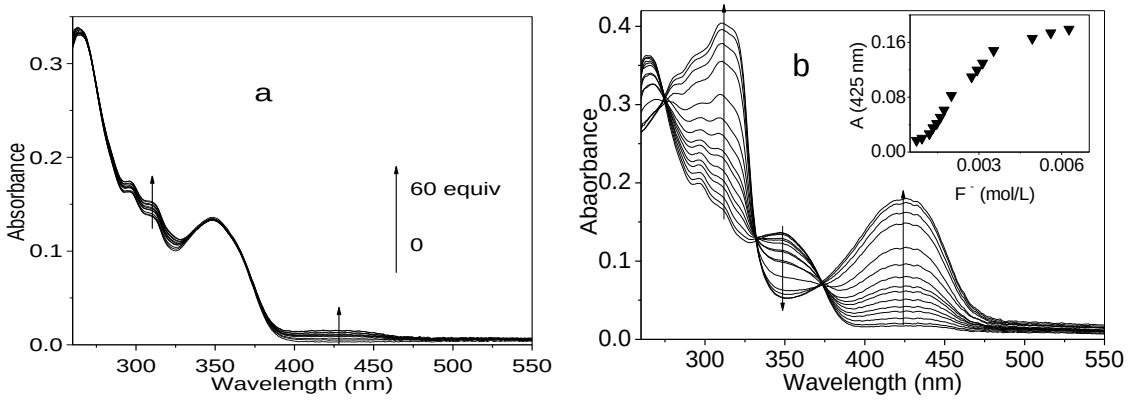

Fig. 2. Change in UV/Vis spectra for PUTO (1.0×10^{-5} M) in DMSO with the addition of $[(Bu)_4N]F$ (a) from 0 to 60 equivalents and (b) from 60 equivalents to 700 equivalents.

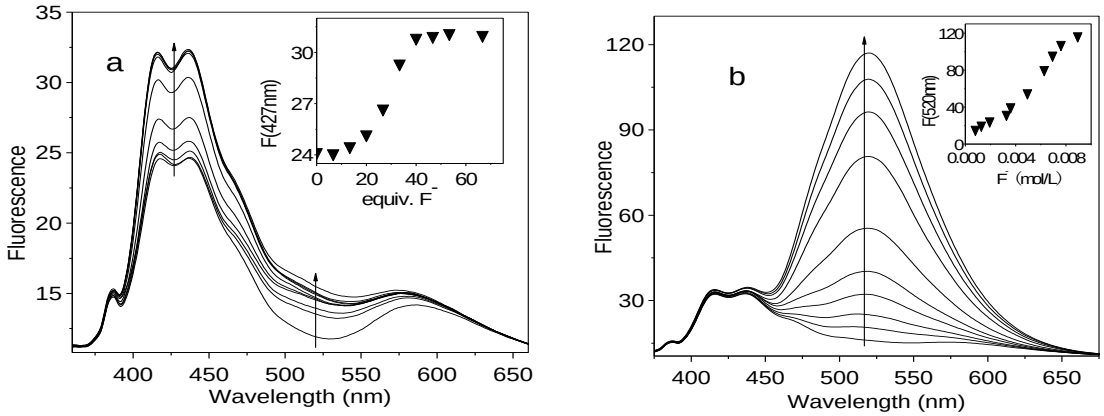

Fig. 3. Change in fluorescent spectra (λex = 331 nm) for PUTO (1.0×10^{-5} M) in DMSO upon the addition of a standard solution of $[(Bu)_4N]F$ (a) from 0 to 60 equivalents and (b) from 60 equivalents to 800 equivalents.

Table 2. The association (log K_a) constants for PUIO interaction with anions

Anion	*Log* K_a[1]	*Log* K_a[2]
F^-	3.28 ± 0.02	3.10 ± 0.02
$CH_3CO_2^-$	2.20 ± 0.14	2.19 ± 0.07
$H_2PO_4^-$	1.96 ± 0.09	1.97 ± 0.05

[1]From UV/Vis titration spectra; and [2]From fluorescence titration spectra.

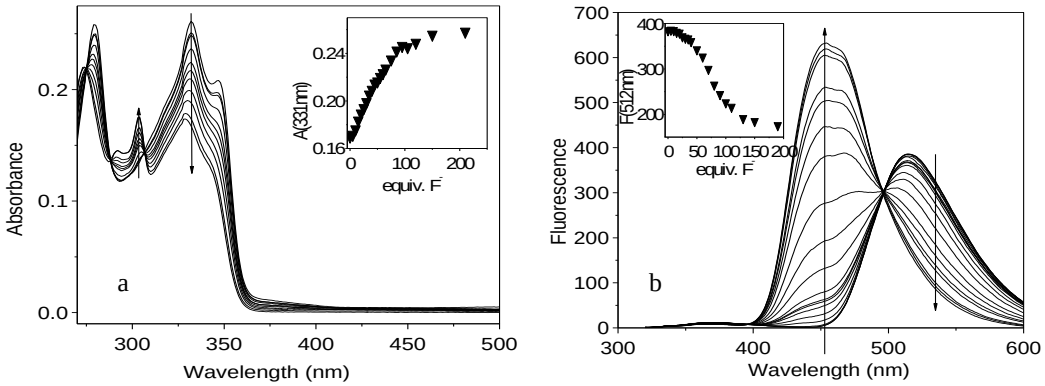

Fig. 4. Change in (a) UV/Vis spectra and (b) fluorescent spectra (λ_{ex} = 306 nm) for PUIO (1.0×10^{-5} M) in DMSO with the addition of the $[(Bu)_4N]F$.

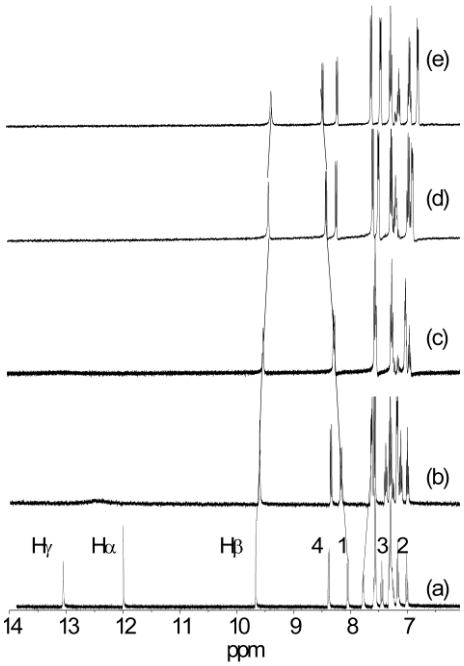

Fig. 5. Partial ^{1}H NMR (400 MHz) spectra of PUIO (1.0×10^{-2} M) in DMSO-d_6 in (a) the absence and (b) the presence of 0.5, (c) 1.0, (d) 2.0, and (e) 4.0 equivalents of $[(Bu)_4N]F$ (proton labeling shown in Scheme 1).

Fig. 6. The color and fluorescence changes of compound PUIO in DMSO (1.0×10^{-4} M) after addition of 50 equivalents $[(Bu)_4N]F$. Left to right: PUIO, PUIO+$[(Bu)_4N]F$, PUIO (emission), and PUIO+$[(Bu)_4N]F$ (emission). Irradiation at 365 nm using a UV lamp.

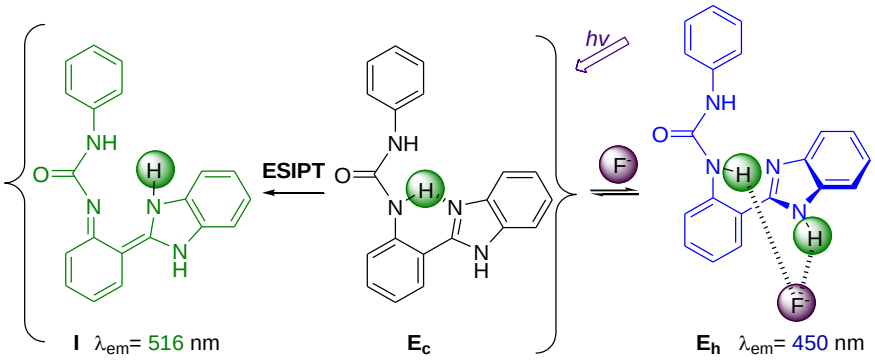

Scheme 6. Inhibition of ESIPT in PUIO by F^-

Spectral titrations were also conducted with the less basic anions such as Cl^-, Br^-, I^-, HSO_4^-, $H_2PO_4^-$ and $CH_3CO_2^-$. Only $CH_3CO_2^-$ and $H_2PO_4^-$ can induce the distinct spectral changes in PUTO and PUIO, but they have less binding affinity to PUTO and PUIO. Specifically, $CH_3CO_2^-$ and $H_2PO_4^-$ induce similar spectral changes in absorbance and fluorescence in PUTO as F^- does. $CH_3CO_2^-$ induces similar spectral changes in absorbance and fluorescence in PUIO as F^- does, but the binding constant for $CH_3CO_2^-$ binding (log K_d = 2.19 ± 0.07) is almost one unit smaller than that for F^- binding (Table 2). While for the less basic anion $H_2PO_4^-$, it induces different spectral changes in PUIO where the intensities of the entire absorption band increase slightly and no isosbestic points are observed during the entire titration, indicating $H_2PO_4^-$ forms very weak hydrogen bonding with PUIO. As for the fluorescent titration spectra, emission band only experiences ~10 nm blue shift with the addition of $H_2PO_4^-$ (not shown), indicating $H_2PO_4^-$ cannot efficiently inhibit the ESIPT process in PUIO.

Conclusions

In conclusion, by replacing the benzoxazole moiety in PUBO with the benzothiazole and benzimidazole, two new ESIPT sensors with relative good detection sensitivity for anions have been developed. Especially for PUIO, the additional -NH binding site of the imidazole ring plays an important role in controlling the mechanism for F^- inhibition of the ESIPT from the deprotonation in PUTO to the hydrogen bonding in PUIO. More importantly, this additional hydrogen bond donor can increase ESIPT efficiency and quantum yields in PUIO and induce a ratiometric response in fluorescence, which makes PUIO being a very sensitive F^- sensors that are based on inhibition of ESIPT mechanism.

Experimental Section

General notes and procedures

^{1}H NMR and ^{13}C NMR spectra were obtained on Varian INVOA 400MHZ spectrometer. Chemical shifts (δ) were reported in ppm relative to Me_4Si standard in DMSO-d_6. HRMS determinations were made on Q-TOF and GC-TOF mass spectrometry (Micromass, England). Steady-state emission spectra were recorded with PTI-700 (corrected) and JASCO FP-6500 (uncorrected) fluorimeter. Absorption spectra were determined on HP8453-Shimadzu UV3100 spectrophotometer. All anions used were F^-, Cl^-, Br^-, I^-, HSO_4^-, $H_2PO_4^-$ and $CH_3CO_2^-$ in the form of their tetrabutylammonium salts.

2-(benzo[*d*]thiazol-2-yl)benzenamine (M1)

Compound M1 was prepared according to a literature method (12). Yield: 95 %; Mp: 125-126 ºC (literature; 126-127 ºC (20)); δ_H (400 MHz; $CDCl_3$; Me_4Si): 6.40 (br, 2H), 6.72-6.79 (m, 2H), 7.19-7.24 (m, 1H), 7.32-7.36 (m, 1H), 7.42-7.46 (m, 1H), 7.69-7.71 (m, 1H), 7.86 (d, 1H, *J* = 8.4 Hz), 7.96 (d, 1H, *J* = 8.4 Hz); δ_C (100 MHz; $CDCl_3$; Me_4Si): 115.6, 117.0, 121.3, 122.6, 124.9, 126.1, 130.5, 131.7, 133.5, 146.9, 154.0, 169.4; HRMS *m*/*z* (Q-TOF MS ES$^+$) calcd for $C_{13}H_{11}N_2S^+$ ([M+H]$^+$), 227.0643, found, 227.0647.

1-(2-(benzo[*d*] thiazole-2-yl)phenyl)-3-phenylurea (PUTO)

Phenyl isocyanate (250 mg, 2.1 mmol) was added to a solution of compound M1 (452 mg, 2 mmol) in dry dioxane (50 mL) in a round flask filled with argon. The mixture was heated at 100 ºC under magnetic stirring for 24 h. After the reaction mixture was cooled to room temperature, a white solid precipitated. Then the crude compound was collected by filtration, dried and recrystallised from dioxane to afford the pure product PUIO as a white solid (552 mg, 80 %). Mp: 260-261 ℃; δ_H (400 MHz; DMSO-d_6; Me_4Si): 7.03 (t, 1H, *J* = 7.2 Hz), 7.19 (t, 1H, *J* = 7.6 Hz), 7.33 (t, 2H, *J* = 8.0 Hz), 7.50-7.64 (m, 5H), 7.93 (d, 1H, *J* = 8.0 Hz), 8.17-8.23 (m, 2H), 8.40 (d, 1H, *J* = 8.4 Hz), 9.76 (s, 1H), 11.19 (s, 1H); δ_C (100 MHz; DMSO-d_6; Me_4Si): 118.9, 119.2, 120.9, 122.0, 122.2, 122.3, 123.1, 125.8, 126.6, 128.7, 130.1, 131.6, 133.1, 138.5, 139.6, 152.6, 167.7; HRMS *m*/*z* (Q-TOF MS ES$^+$) calcd for $C_{20}H_{15}N_3NaSO^+$ ([M+Na]$^+$), 368.0834, found, 368.0831.

2-(benzo[*d*]imidazol -2-yl)benzenamine (M2)

Compound M2 was also prepared according to a literature method (12). Yield: 60 %; Mp: 209-210 ºC (literature; 213-214 ºC (27)); δ_H (400 MHz; DMSO-d_6; Me_4Si): 6.65 (t, 1H, *J* = 7.2 Hz), 6.82 (d, 1H, *J* = 8.0 Hz), 7.13-7.24 (m, 5H), 7.49 (d, 1H, *J* = 7.6 Hz), 7.64 (d, 1H, *J* = 7.2 Hz), 7.82 (d, 1H, *J* = 8.0 Hz); δ_C (100 MHz; $CDCl_3$; Me_4Si): 110.1, 110.7, 114.9, 116.1, 118.1, 121.4, 122.3, 127.2, 130.4, 143.0, 148.2, 152.5; HRMS *m*/*z* (GC-TOF MS ES$^+$) calcd for $C_{13}H_{11}N_3^+$ ([M]$^+$), 209.0952, found, 209.0953.

1-(2-(benzo[*d*]imidazol-2-yl)phenyl)-3-phenylurea (PUIO)

Phenyl isocyanate (250 mg, 2.1 mmol) was added to a solution of compound M2 (418 mg, 2 mmol) in dry dioxane (50

mL) in a round flask filled with argon. The mixture was heated at 100 °C under magnetic stirring for 24 h. After the reaction mixture was cooled to room temperature and evaporated to dryness. The crude compound was purified by flash column chromatography on silica gel (1:1 dichloromethane/EtOAc) to afford a white solid. Yield: 80 %; Mp > 280 °C; δ_H (400 MHz; DMSO-d_6; Me_4Si): 7.01 (t, 1H, *J* = 7.2 Hz), 7.16 (t, 1H, *J* = 7.6 Hz), 7.23-7.32 (m, 4H), 7.45 (d, 1H, *J* = 8.0 Hz), 7.55-7.59 (m, 3H), 7.77 (d, 1H, *J* = 7.2 Hz), 8.04 (d, 1H, *J* = 8.0 Hz), 8.38 (d, 1H, *J* = 8.4 Hz), 9.64 (s, 1H), 11.98 (s, 1H), 13.04 (s, 1H); δ_C (100 MHz; DMSO-d_6; Me_4Si): 111.3, 115.2, 118.8, 119.3, 120.4, 121.3, 121.9, 122.1, 123.2, 127.3, 128.6, 130.2, 133.6, 139.3, 139.8, 142.3, 151.0, 152.8; HRMS *m*/*z* (GC-TOF MS ES$^+$) calcd for $C_{20}H_{16}N_4O^+$ ([M]$^+$), 328.1324, found, 328.1326.

Determination of quantum yields

Quantum yields were determined by the relative comparison procedure. The absorption band maxima of standard and unknown samples were adjusted below 0.1. Corrected emissions were recorded with a PTI-700 fluorimeter for quantum yields determination (emission correction file provided by instrument manufacturer). The quinine sulfate with the quantum yields of 0.51 in sulfuric acid (0.05 M) was used as the standard. The general equation used in the determination of relative quantum yields is shown as follows:

$$Q_u = \frac{Q_s \times F_u \times A_s \times \lambda_{exs} \times \eta_u^2}{F_s \times A_u \times \lambda_{exu} \times \eta_s^2}$$

Where *Q* is the quantum yields; *F* is the integrated area under the corrected emission spectrum; *A* is the absorbance at the excitation wavelength; *ex* is the excitation wavelength; η is the refractive index of the solution; and the subscripts *u* and *s* refer to the unknown and the standard, respectively

Determination of dissociation constant

Equilibrium constant was fitted 1:1 model for substrate-ligand interactions. For example, if the UV/Vis titration spectra are used for the equilibrium constants determination, the binding isotherm is shown as follows:

$$\frac{\Delta A}{b \times S \times \Delta\varepsilon} = \Delta A_N = \frac{K \times [L]}{1 + K \times [L]}$$

Where *A* is the absorbance; *b* is the length of sample cell; *S* is the total concentration of substrate; ε is extinction coefficients; ΔA_N is the normalized absorbance changes $\Delta A/(A_{max}-A_{min})$; *K* is the equilibrium constants; [*L*] is the free ligand concentration and the approximation $[L] \approx L$ is made. The semilogarithmic plots of ΔA_N against -log[*L*] fitted with Sigmoidal give log*K* for sensor interaction with anion.

Conflict of Interest: None

Acknowledgements

This work was supported by the National Natural Science Foundation of China (Nos. 21576037, 21422601, 21421005, and U1608222), NSFC-Liaoning United Fund (No. U1608222).

References

1. Arnaut LG, Formosinho SJ. Excited-state proton transfer reactions. I. Fundamentals and intermolecular reactions. J Photochem Photobiol A: Chem 1993; 75(1):1-20.
2. Formosinho SJ, Arnaut LG. Excited-state proton transfer reactions. II. Intramolecular reactions. J Photochem Photobiol A: Chem 1993; 75(1):21-48.
3. Obare SO, Murphy CJ. Selective blue emission from an HPBO-Li+ complex in alkaline media. New J Chem 2001; 25(12):1600-4.
4. Wu KC. Lin YS, Yeh YS, Chen CY, Ahmed MO, Chou PT, Hon YS. Design and synthesis of intramolecular hydrogen bonding systems. Their application in metal cation sensing based on excited-state proton transfer reaction. Tetrahedron 2004; 60(51):11861-8.
5. Taki M, Wolford JL, O'Halloran TV. Emission ratiometric imaging of intracellular zinc: Design of a benzoxazole fluorescent sensor and its application in two-photon microscopy. J Am Chem Soc 2004; 126(3):712-3.
6. Henary MM, Wu YG, Fahrni CJ. Zinc(II)-selective ratiometric fluorescent sensors based on inhibition of excited-state intramolecular proton transfer. Chem Eur J 2004: 10(12):3015-25.
7. Zhang XB, Peng J, He CL, Shen GL, Yu RQ. A highly selective fluorescent sensor for Cu2+ based on 2-(2'-hydroxyphenyl)benzoxazole in a poly(vinyl chloride) matrix. Anal Chim Acta 2006; 567(2):189-95.
8. Tong H, Zhou G, Wang LX, Jing XB, Wang FS, Zhang JP. Novel highly selective anion chemosensors based on 2,5-bis(2-hydroxyphenyl)-1,3,4-oxadiazole. Tetrahedron Lett 2003; 44(1):131-4.
9. Lee JK, Na JH, Kim TH, Kim YS, Park WH, Lee TS. Synthesis of polyhydroxybenzoxazole-based colorimetric chemosensor for anionic species. Mater Sci Eng C 2004; 24(1-2):261-4.
10. Schrader T, Hamilton AD. Functional Synthetic Receptors, Wiley-VCH: Weinheim 2005.
11. Sessler JL, Cho WS, Gale PA. Anion Receptor Chemistry, RSC 2006.
12. Wu FY, Li Z, Guo L, Wang X, Lin MH, Zhao YF, Jiang YB. A unique NH-spacer for N-benzamidothiourea based anion sensors. Substituent effect on anion sensing of the ICT dual fluorescent N-(p-dimethylaminobenzamido)-N'-arylthioureas. Org Biomol Chem 2006; 4(4):624-30.
13. Gunnlaugsson T, Ali HDP, Glynn M, Kruger PE, Hussey GM, Pfeffer FM, dos Santos CMG, Tierney J. Fluorescent photoinduced electron transfer (PET) sensors for anions; From design to potential application. J Fluores 2005; 15(3):287-99.
14. Gunnlaugsson T, Glynn M, Tocci GM, Kruger PE, Pfeffer FM. Anion recognition and sensing in organic and aqueous media using luminescent and colorimetric sensors. Coord Chem Rev 2006; 250:3094-117.
15. Sun SS, Anspach JA, Lees AJ, Zavalij PY. Synthesis and electrochemical, photophysical, and anion binding properties of self-assembly heterometallic cyclophanes. Organometallics 2002; 21(4):685-93.
16. Wu JS, Zhou JH, Wang PF, Zhang XH, Wu SK. New fluorescent chemosensor based on exciplex signaling mechanism. Org Lett 2005; 7(11):2133-6.
17. Peng XJ, Wu YK, Fan JL, Tian MZ, Han KL. Colorimetric and ratiometric fluorescence sensing of fluoride: Tuning

selectivity in proton transfer. J Org Chem 2005; 70(25):10524-31.
18. Wu YK, Peng XJ, Fan JL, Gao S, Tian MZ, Zhao JZ, Sun S. Fluorescence sensing of anions based on inhibition of excited-state intramolecular proton transfer. J Org Chem 2007; 72(1):62-70.
19. Henary MM, Fahrni CJ. Excited state intramolecular proton transfer and metal ion complexation of 2-(2'-hydroxyphenyl)benzazoles in aqueous solution. J Phys Chem A 2002; 106(21):5210-20.
20. Hein DW, Alheim RJ, Leavitt JJ. The use of polyphosphoric acid in the synthesis of 2-aryl- and 2-alkyl-substituted benzimidazoles, benzoxazoles, and benzothiazoles. J Am Chem Soc 1957; 79:427-9.
21. Santra S, Krishnamoorthy G, Dogra SK. Excited-state intramolecular proton transfer in 2-(2'-acetamidophenyl)benzimidazole. J Phys Chem A 2000; 104(3):476-82.
22. Martinez-Manez R, Sancenon F. Fluorogenic and chromogenic chemosensors and reagents for anions. Chem Rev 2003; 103(11):4419-76.
23. Gomez DE, Fabbrizzi L, Licchelli M, Monzani E. Urea *vs*. thiourea in anion recognition. Org Biomol Chem 2005; 3(8):1495-500.
24. Han F, Bao YH, Yang ZG, Fyles TM, Zhao JZ, Peng XJ, Fan JL, Wu YK, Sun SG. Simple bisthiocarbonohydrazones as sensitive, selective, colorimetric, and switch-on fluorescent chemosensors for fluoride anions. Chem Eur J 2007; 13(10):2880-92.
25. Amendola V, Boiocchi M, Fabbrizzi L, Palchetti A. Anion receptors containing NH binding sites: Hydrogen-bond formation or neat proton transfer? Chem Eur J 2004; 11(1):120-7.
26. Valeur B. Molecular Fluorescence: Principles and Applications, Wiley-VCH 2001, 1 edition.
27. Zaika LL, Joullie MM. 1,2,3-Benzotriazines. I. The synthesis of some benzimidazo[1,2-c][1,2,3]benzotriazines and naphth[1',2'(2',1'):4,5]imidazo[1,2-c][1,2,3]benzotriazine. J Heterocyclic Chem 1966; 3:289-98.